

**ESDA2010-24031**

**ENHANCEMENT POTENTIAL OF THE THERMAL CONVERSION EFFICIENCY OF ICE CYCLES BY USING OF A REAL ATKINSON CYCLE IMPLEMENTATION AND (VERY) HIGH PRESSURE TURBO CHARGING**

**Victor GHEORGHIU, Prof. PhD ME**  
 Hamburg University of Applied Sciences,  
 Berliner Tor 21, 20099 Hamburg, Germany  
 E-mail: victor.gheorghiu@haw-hamburg.de

**ABSTRACT**

Most recent implementations of the Atkinson cycle are not optimal from the point of view of Thermal Conversion Efficiency (TCE). For example, Toyota has put in its Prius II a gasoline engine which should achieve high efficiency by using a modified Atkinson cycle based on variable intake valve timing management. Firstly, this implementation of the Atkinson cycle is not the optimal solution because some of the air is first sucked from the intake manifold into the cylinder and subsequently returned back there. As a consequence, the oscillating air stream considerably reduces the thermal conversion efficiency of this cycle. Secondly, this implementation of the Atkinson cycle reaches only low levels of Indicated Mean Pressure (IMEP) and, thirdly, it is not suitable for part load Engine Operating Points (EOP) because of the lower TCE. For these reasons, this implementation of the Atkinson cycle is suitable only for hybrid vehicles, where the engine - because it is not directly linked mechanically to the wheels - works only in its best EOP.

In this paper the losses in TCE of Internal Combustion Engine (ICE), especially for the Atkinson cycles, are analyzed in detail and a proposal is made for their reduction for aspirated and especially for high pressure supercharged engines.

**INTRODUCTION**

The principal purpose of this investigation is to discover new ways for implementing the Atkinson cycle, which simultaneously enables the enhancement of TCE and IMEP under stoichiometric AFR and lower pressure and temperature peaks during the cycle.

In conventional ICE, because the volumetric compression and expansion strokes are virtually identical and the cylinder

filling is complete, the effective compression ratio and the effective expansion ratio are basically identical, as shown on the left side of Fig. 1, for the modified Seiliger cycle (an ideal model of engine cycles).

In the classic Seiliger cycle [2], or limited pressure cycle [1] the heat is released by constant volume (V) and constant pressure (p). For this reason, this cycle is referred to here as the V, p-cycle. In the modified Seiliger cycle, (see left side of Fig. 1) the heat is released by constant volume, constant pressure and constant temperature and, accordingly, this cycle can be referred to as the V, p, T-cycle. In this way, it becomes possible to generate ideal cycles which model the real ICE cycles more accurately by observing their mechanical and thermal limits.

In the Atkinson cycle (see right side of Fig. 1), the effective compression stroke is shorter and the effective compression ratio is higher than those of the Seiliger cycle, so that the pressure at the end of the compression strokes reaches the same level in both cycles. In this case, the Atkinson cycle has a higher TCE than the Seiliger cycle.

The following operations are the usual ways (see [1], [2]) to increase the TCE of the Seiliger cycle:

1. Increasing the effective volumetric compression ratio (VCR).
2. Shortening the effective compression stroke, for example by delaying intake valve closing.
3. Completing the effective expansion stroke, for example by delaying the exhaust valve opening.
4. Enhancement of turbocharging level for a concurrent increase in TCE and indicated mean pressure (IMEP).

In conclusion, these ways of increasing the TCE of the classic Seiliger cycle (marked by arrows on the left side of Fig. 1) lead to both aspirated and turbocharged engines from

Seiliger to Atkinson cycle and result in the following implications, limitations and restrictions:

The first and fourth ways lead to higher pressure and temperature peaks during the cycle, which increase the thermal and mechanical strain on engine parts. The occurrence of knocking is a frequent outcome in the case of gasoline engines. The high temperature favors the production of NOx in the cylinders of both gasoline and diesel engines. The second way leads to a decreased mass of retained gas in the cylinder, especially in the case of aspirated engines.

As a consequence, the IMEP achieves only low levels and engines with a higher displacement are necessary, the mechanical losses rise, and, finally, the increase in TCE is lost. The third way leads to engines with large displacement and consequently higher mechanical losses, when the volumetric expansion stroke increases while the compression stroke remains unchanged.

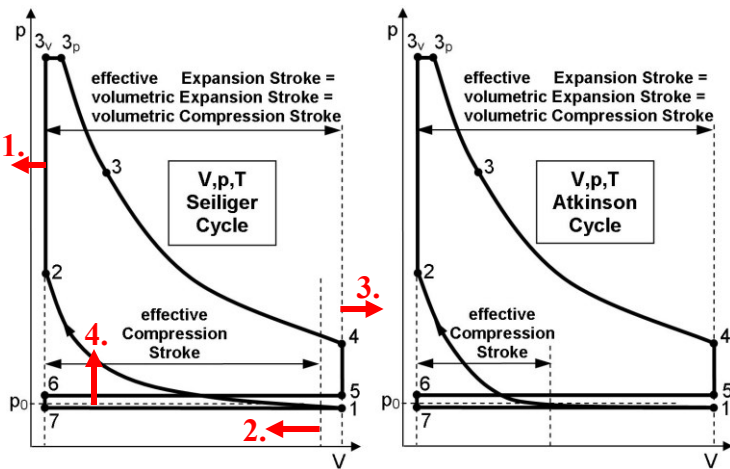


Figure 1. Schematic Pressure-Volume diagrams of classic four-stroke Seiliger and Atkinson cycle

## 1. ATKINSON CYCLE IMPLEMENTATIONS TO ICE WITH CLASSIC CRANKSHAFT DRIVE

### 1.1 Analysis of Atkinson Cycle Implementation for Aspirated ICE in Variant 2V

For example, Toyota uses an SI engine in its Prius II which tries to achieve high efficiency by using an Atkinson cycle, where the intake valve is kept open for a large part of the compression stroke and the volumetric compression ratio is enhanced [3].

This implementation of the Atkinson cycle (named second variant or 2V) is compared with the classic Seiliger cycle (named standard variant or SV), and the results are presented in Figures 2 to 5. The third implementation variant of Atkinson cycle (3V) drawn in these Figures will be presented and discussed below. These three variants are described and evaluated in detail in [4] by using the simulation method and tool presented in [5] and [6]. In these variants, the air-fuel ratio

(AFR) is kept stoichiometric, the cylinder walls are adiabatic and the thermo and fluid dynamical processes are reversible to make comparison easier.

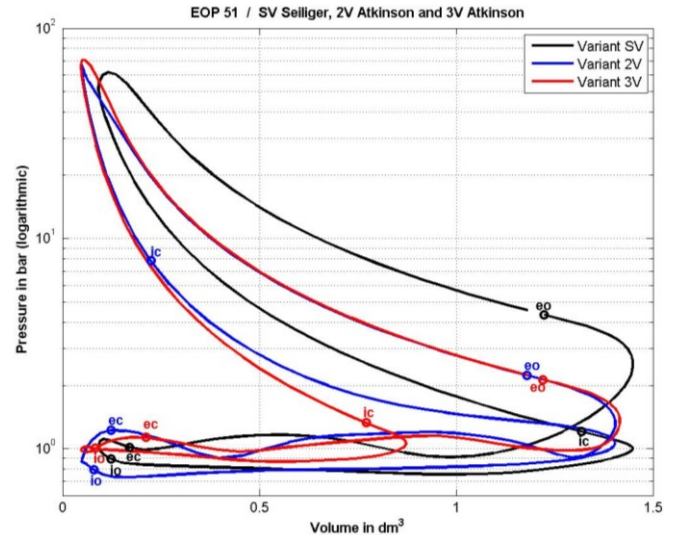


Figure 2. Pressure (Logarithmic) - Volume Diagram

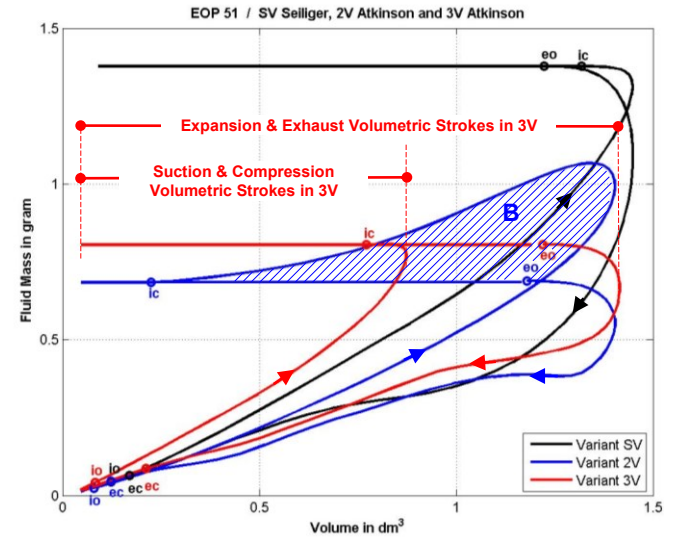
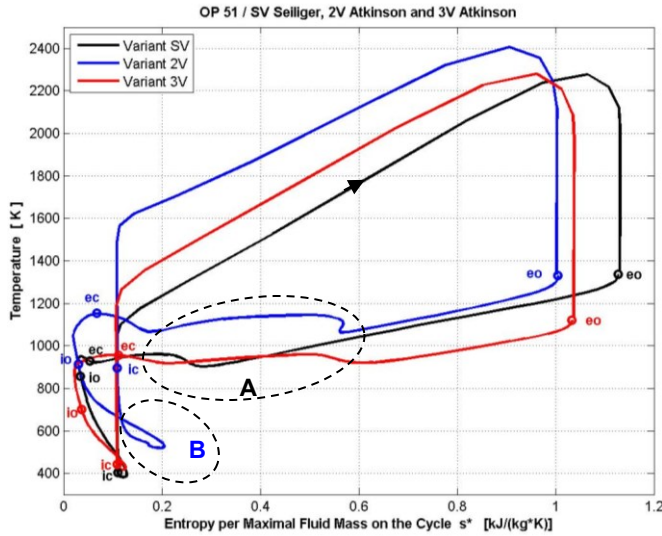


Figure 3. Fluid Mass-Volume Diagram

In the initial stage of the compression stroke in 2V, due to the delayed intake valve close (ic), some of the air that had entered the cylinder is returned to the intake manifold, in effect delaying the start of compression (see B areas in Fig. 3 and 4). In this way, the effective compression ratio is decreased without altering the expansion ratio. The oscillating air stream from and to the intake manifold through the intake valve port considerably reduces the TCE and the indicated fuel conversion efficiency (IFCE) of the cycle (see B areas in Fig. 4 and 5). The pushing out of residual gases during the exhaust stroke consumes more piston work in the Atkinson cycle because of lower pressure (see Fig. 2) at the exhaust valve opening (eo)

and consequently of the sluggish cylinder emptying (see **A** areas in Fig. 4 and 5).



**Figure 4.** Temperature-specific\* Entropy (Entropy per Maximal Fluid Mass on the Cycle) Diagram (T, s\*)

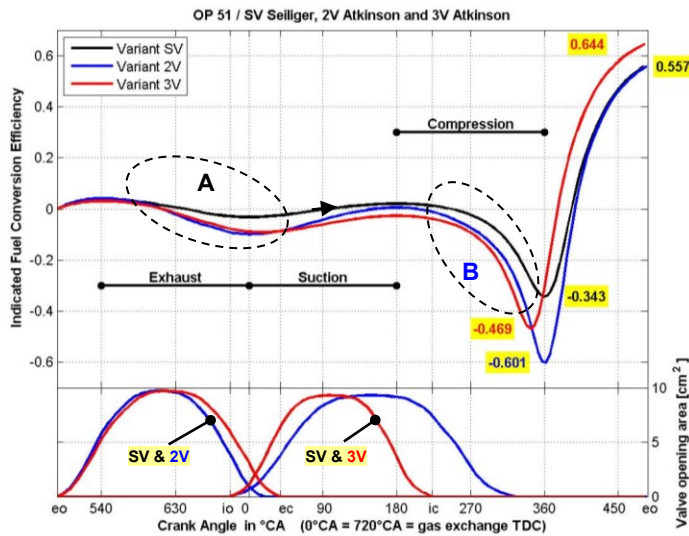


**Figure 5.** IFCE – Crank Angle Diagram

One can conclude that the TCE gain of this kind of Atkinson cycle implementation (i.e. **2V**) is modest and largely dependent on the fine-tuning of all parameters (valve timing, etc.). The major TCE improvement in the case of Prius II is obtained by means of sifting the EOP in areas with greater TCE. In addition, the specific power or IMEP of the engine is low because of the lower retained mass of fresh charge in cylinder before compression (see Fig. 3). This means a relatively large (due to the large displacement) and therefore heavy engine is needed to power the vehicle.

For these reasons, this implementation of the Atkinson cycle is suitable only for hybrid vehicles, where the engine – because it is not directly linked mechanically to the wheels – works only in its best operating range [3].

## 1.2 Analysis of Classic Atkinson Cycle Implementation for Supercharged ICE in the Variant 1V-TC

First, the commonly used practice of concomitant suction delaying and increase in boost pressure is analyzed. The number of parameters influencing the TCE of supercharged engines becomes much higher compared to aspirated engines. As a consequence, the effort to achieve combinations of parameters which maximize the TCE of such engine cycles becomes much bigger.

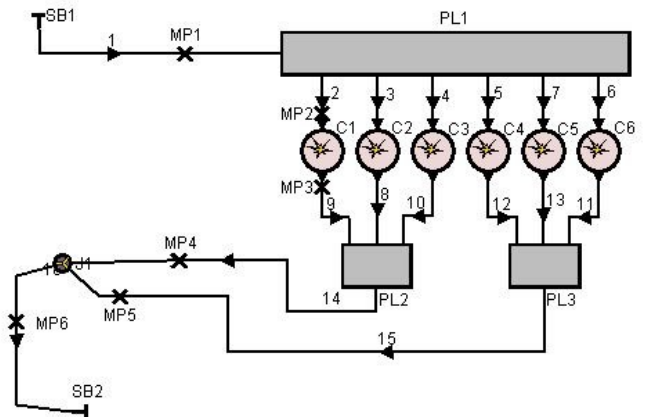


**Figure 6.** Simple BOOST model of a supercharged 6-cylinder diesel engine

The simulation tool used here is the BOOST<sup>®</sup>, from AVL Co. The BOOST model used for the following implementations is presented in Figure 6, where the six cylinders of the modeled engine are identical.

The following options were selected for the BOOST models of the Seiliger and Atkinson cycles:

- The goal is to reach the greatest possible TCE and the indicated mean pressure at the same time, without exceeding the given mechanical and thermal limits.
- The VCR for both cycles is kept identical.
- The heat transfer to the cooling system is switched off in order to enable an easier comparison between cycles and variants, as done previously in [8].
- The heat release function is modeled with the help of a simple Vibe function (identical for all simulations).
- The mechanical and thermal limits are kept identical (ca. 210 bar respective 2,050 K) in both cycles and all of the simulation variants, as done previously in [8].
- In order to reach the same limits for pressure and temperature in both cycles, the charge pressure  $p_c$  is adjusted accordingly.
- The air-fuel ratio ( $\lambda$  or **AFR**) is kept identical in order to compare the cycles using the same load.



- The charge temperature is kept identical for all simulations ( $T_c = 350$  K), as done previously in [8].
- The supercharging level is simulated by setting the state of the boundary element SB1 and the pressure before the turbine by setting the state of the boundary element SB2 (see Fig. 6). In this instance, the turbocharger and the intercooler are no longer required to be modeled in detail and, in addition, the comparability is assured between various simulations for both cycles.
- The parameters compared here are TCE ( $\eta_{th}$ ), IMEP ( $p_i$ ), retained mass in cylinder ( $m_a$ ) and pressure ( $p_{ic}$ ), and also the temperature ( $T_{ic}$ ) when the intake valve closes (**ic**) in both cycles.

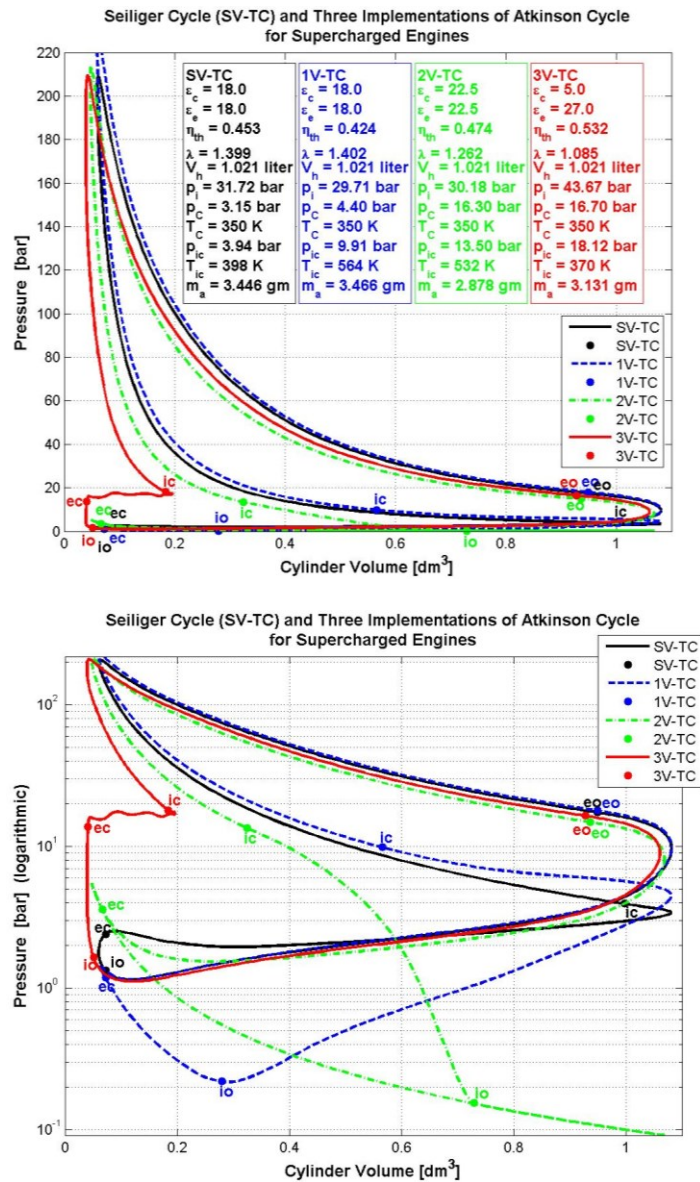


Figure 7. Pressure-Volume Diagrams

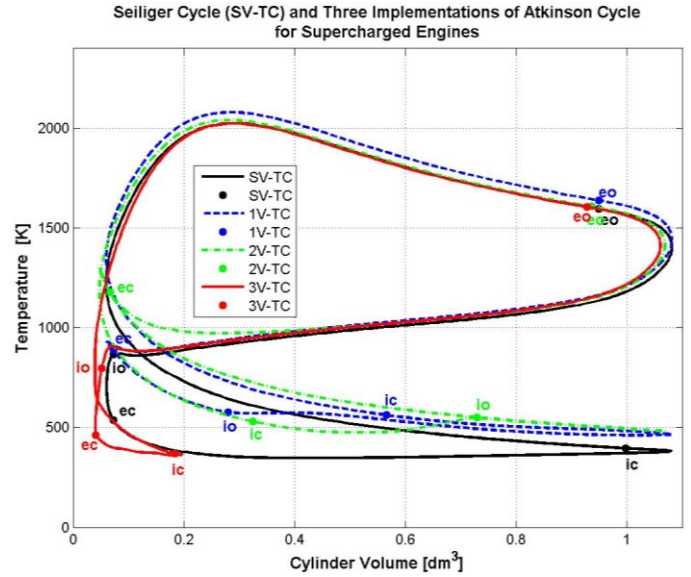


Figure 8. Pressure-Temperature Diagrams

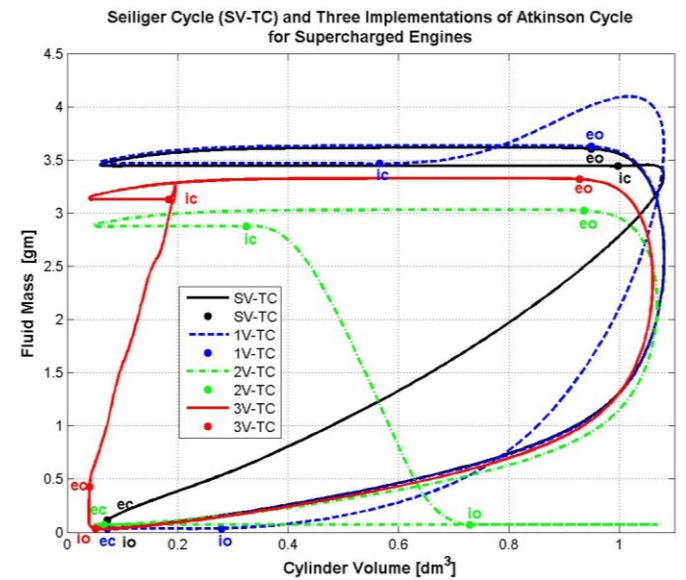


Figure 9. Fluid Mass-Volume Diagrams

The simulation results for the 1V-TC of Atkinson cycle implementation, where the intake valve closing is  $60^\circ$ CA delayed, are presented in Figures 7 to 10. Due to the delay in suction, the gas exchange processes are very different from the SV-TC of the Seiliger cycle. The boost in pressure is increased by the same filling rate of the cylinder (see Fig. 9) to achieve nearly the same IMEP.

At the beginning of the intake stroke, the pressure in the cylinder decreases significantly because the intake valve is not yet open at this time (see Fig. 7). The IFCE level is therefore lower than in the SV-TC (see Fig. 10). Toward the end of suction, when the return flow is carried to the inlet pipe (see

Fig. 9 and 10), the IFCE level becomes much lower than in the standard version (see Fig.10).

In short, although in the **1V-TC** of the Atkinson cycle implementation the boost pressure is 40% higher, TCE or IFCE and IMEP are 6% lower than in the standard version of the Seiliger cycle. For these reasons, a new approach is needed to implement the Atkinson cycle with a normal crankshaft drive.

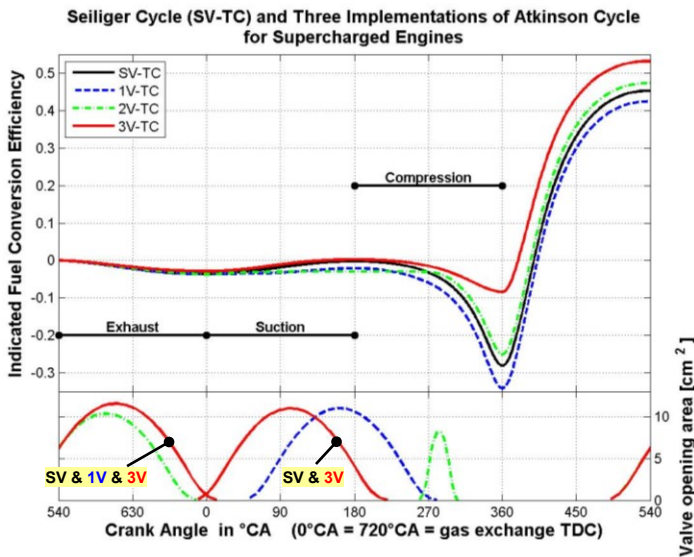


**Figure 10.** IFCE-Crank Angle Diagrams

As a following attempt here a test should be done on the IFCE improvement potential of an engine where a very high-pressure supercharging and a high value of the VCR are used simultaneously. The usual reduction of the VCR for meeting the mechanical and thermal limitations, when very high-pressure supercharging is used for an engine with classic crank drive, implies diminishing IFCE performance.

### 1.3 Analysis of Atkinson Cycle Implementation with Very High Charge Pressure in Variant 2V-TC

In the **2V-TC** implementation of the Atkinson cycles, the suction is much more delayed and a very high charge pressure (of more than 16 bars) is considered. As a result of the delayed suction, less mass is aspirated into the cylinder (see Fig. 9). To improve the IFCE of this Atkinson cycle, the VCR is increased by 22% compared to the **SV-TC** of the Seiliger cycle.

The special characteristics of the **2V-TC** are: a) the remaining gases are expanded during suction stroke and then compressed as in the Miller cycle (see e.g. [7]) and b) the suction of fresh charge starts first, after the full completion of the suction in the **SV-TC**, and takes a very short time.

Unfortunately, in order to achieve the same maximum values of pressure and temperature on both cycles at virtually the same IMEP, the AFR must be adapted in this case. The placement of the combustion phase on the cycle is identical to the **SV-TC** of the Seiliger cycle. The simultaneous matching of all the parameters (i.e. maximum values of pressure and

temperature, IMEP and AFR) is very difficult to achieve. The difference between the AFR ( $\lambda$ ) values of both cycles (see parameter boxes from Fig. 7) is quite low.

During exhaust, there are no major differences in IFCE between the cycles (see Fig. 10). The significant influence of the decrease in compression work in the **2V-TC** of Atkinson cycle can be seen clearly after the intake valve is closed.

In short, it can be seen that this implementation of the Atkinson cycle is somewhat more efficient than the Seiliger cycle. One can expect that the improvement in IFCE for the **2V-TC** of Atkinson cycle, compared to the standard Seiliger cycle, will be somewhat better if the AFR is kept identical in both cycles. Although the boost pressure in the **2V-TC** of Atkinson cycle implementation is more than five times higher at nearly the same IMEP, one sees only a minor improvement in the IFCE. Hence, the implementation of the Atkinson cycle by means of a significant delay of the suction and a strong enhancement of the charge pressure applied to a classic Seiliger cycle does not represent a suitable solution. Therefore, a new approach is needed to implement a **real Atkinson cycle**.

## 2. STRICT ATKINSON CYCLE IMPLEMENTATIONS TO ICE WITH ASYMMETRICAL CRANKSHAFT DRIVE

The goal of the present investigation is to attempt to propose better implementations of the Atkinson cycle in accordance with the previously presented restrictions.

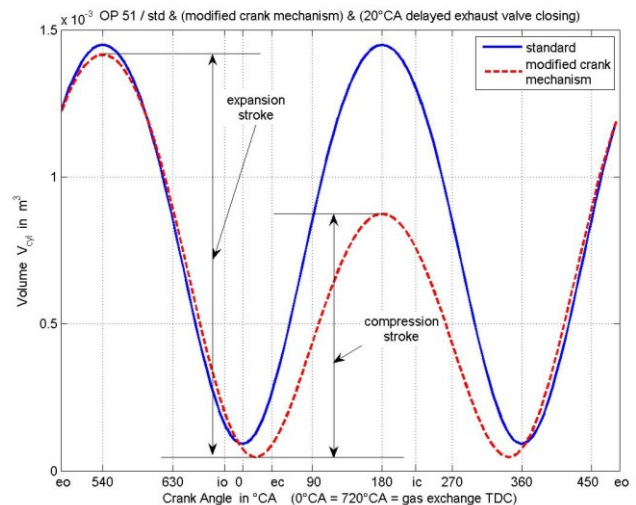


**Figure 11.** Relative Piston Displacement – CA Diagram of an Asymmetrical Crank Mechanism with Constant VCR for an Aspirated Engine [4]

In order to realize a strict Atkinson cycle - i.e. shortened compression and extended expansion - a special crankshaft drive is proposed which permits geometrically different strokes for compression and expansion (see Fig. 11 for aspirated engines [4] and Fig. 12 for supercharged engines [8]). The design of this crankshaft drive is not the subject of this

investigation and is therefore not described here. Its mechanical efficiency is estimated to be more than 96%. Many crank mechanisms with asymmetrical strokes are already patented in several variants, or have reached the stage of application for a patent.

## 2.1 Analysis of Atkinson Cycle Implementation for Aspirated ICE in Variant 3V

An analysis of the simulation results from [4] for the implementation of a real Atkinson cycle in 3V shows that a 15% increase in IFCE (see Fig. 5) can be achieved in comparison to the standard Seiliger cycle (SV). The backflow to the intake manifold through the intake valve port at the beginning of compression can be eliminated with shortened suction and compression strokes (see Fig. 3). An analysis of the  $T_s^*$  diagrams from Figure 4 reveals why the TCE or IFCE are higher in the 3V than in the 2V and SV variants. The only factor which could have contributed to this is the elimination of the back and forth streaming through the intake valve, since no other changes or parameter optimizations were made compared to the 2V of Atkinson cycle implementation.

## 2.2 Analysis of Atkinson Cycle Implementation to ICE with Very High Charge Pressure in Variant 3V-TC

In the SV-TC implementation of the Seiliger cycle the expansion and compression ratios are identical. In the 3V-TC implementation of the Atkinson cycle, the crank mechanism from Figure 12 in Position 3, the chosen parameters are a very low compression ratio, a very high boost pressure  $p_c$  and a virtually stoichiometric AFR ( $\lambda$ ) (see parameter boxes from Fig. 7 for this variant). In this way, the full potential of turbo charging can be used without exceeding the maximum pressure (in this case  $p_{\max} = 210$  bar) and temperature (in this case  $T_{\max} = 2050$  K) of the cycle (see Fig. 7 to 9).

The charge pressure in the 3V-TC implementation of the Atkinson cycle is unusually high. Such turbo charging systems are not typical at this time for ICE because the maximum pressure on the cycle severely limits the level of charge pressure in classic applications (here SV-TC). For this reason, the current classic, highly supercharged diesel engines must decrease sharply either the VCR or the aspirated air mass (classic Atkinson and Miller cycle, see e.g. [7]) in order to avoid exceeding the maximum pressure during the cycle. These restrictive measures limit the TCE or IFCE of these cycles substantially.

Consequently, our search in this paper has been for ways to make better use of the enthalpy of exhaust gases. In the case of stoichiometric AFR this enthalpy is more than enough to provide the compression of the fresh charge up to the very high pressure ( $p_c$ ) of the 3V-TC of the Atkinson cycle implementation from Figures 7 to 10. On the other hand, the temperature of the fresh charge ( $T_c$ ) must be kept low by means of intensive cooling after each turbo compressor stage. The high level of  $p_c$ , the low level of  $T_c$  and the reduced piston work for compression considerably increase the TCE or IFCE on this

Atkinson cycle. In addition, the piston work for gas exchange processes becomes very positive, i.e. this piston work is supplied for this Atkinson cycle implementation instead of being consumed as in the case of the SV-TC of Seiliger cycle (see Fig. 7 and 10).

As a result, the TCE of the 3V-TC of the Atkinson cycle is more than 17% greater than that of the SV-TC of the Seiliger cycle. At the same time, the indicated mean pressure ( $p_i$  or IMEP) of the 3V-TC of the Atkinson cycle exceeds that of the SV-TC of Seiliger cycle by more than 37%, while meeting the same mechanical and thermal limits in both cycles (see Fig. 7 to 10). It should be noted here that as the AFR cannot be kept identical in both simulated cycles, these cycles correspond to different engine operating conditions. As a consequence, the effort to achieve combinations of parameters which maximize the TCE of the real ICE cycle of supercharged engines, while keeping identical thermal and mechanical limits, AFR respectively operating condition, charge pressure and temperature etc. becomes much more difficult.

Consequently, **ideal models of the  $V_p, T$ -Seiliger and -Atkinson cycles** are developed for this purpose (see Appendix [8] for theoretical background). Simulations with BOOST (as **real models** of ICE cycles) are used in [8] for reference in order to evaluate the accuracy and validate the prediction accuracy of these **ideal models** on the TCE. The purpose of the BOOST simulations from [8] was not to obtain a perfect overlapping of the curves, but rather to demonstrate that the proposed  $V_p, T$ -model is able to produce good results and accurate predictions of the influence that many parameters have on the TCE without a major computing effort.

## 2.3 Analysis of Atkinson Cycle Implementations to ICE with Very High Charge Pressure over all EOP using the Ideal $V_p, T$ - Model

The implementation of the Atkinson cycle by means of the asymmetrical crank drive has the disadvantage that at part loads - because of the very extensive expansion - the cycle stops being feasible, i.e. the pressure at the end of expansion becomes lower than the ambient pressure (see Appendix, Requirements for cycle realization). For this reason, the crank drive should also enable the variation of the VCR, as presented in Figure 12.

Using such a crank mechanism it is possible to realize Atkinson cycles for part loads even with stoichiometric AFR and without throttling. For example, the pressure-volume, temperature-volume, fresh charge mass-volume and temperature-specific entropy diagrams for Position 1 of the crank mechanism (see Fig. 12) at full and many part loads are presented in Figure 13. The best TCE is reached for a boost pressure of ca. 10 bar.

For this position of the crank mechanism and for the stoichiometric AFR the limits for the boost pressure are between 2 and 34 bar. For the other positions of the crank mechanism, these limits are different. These boost pressure limits are set by requirements 1 to 5 for cycle realization and the formula for the ideal  $V_p, T$  model (see Appendix).



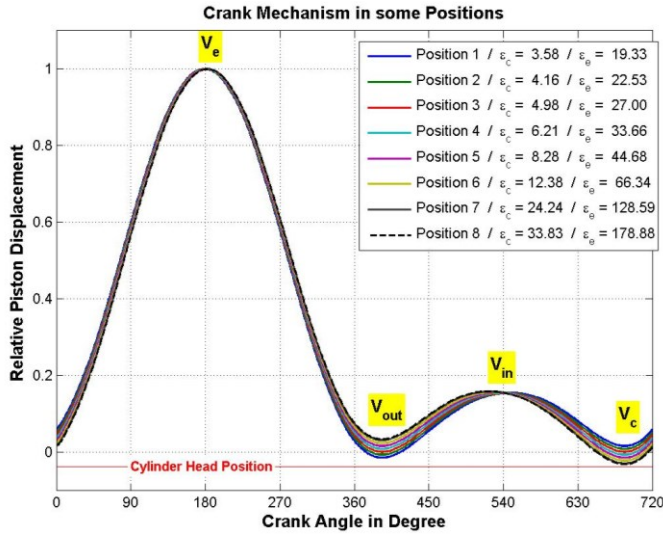


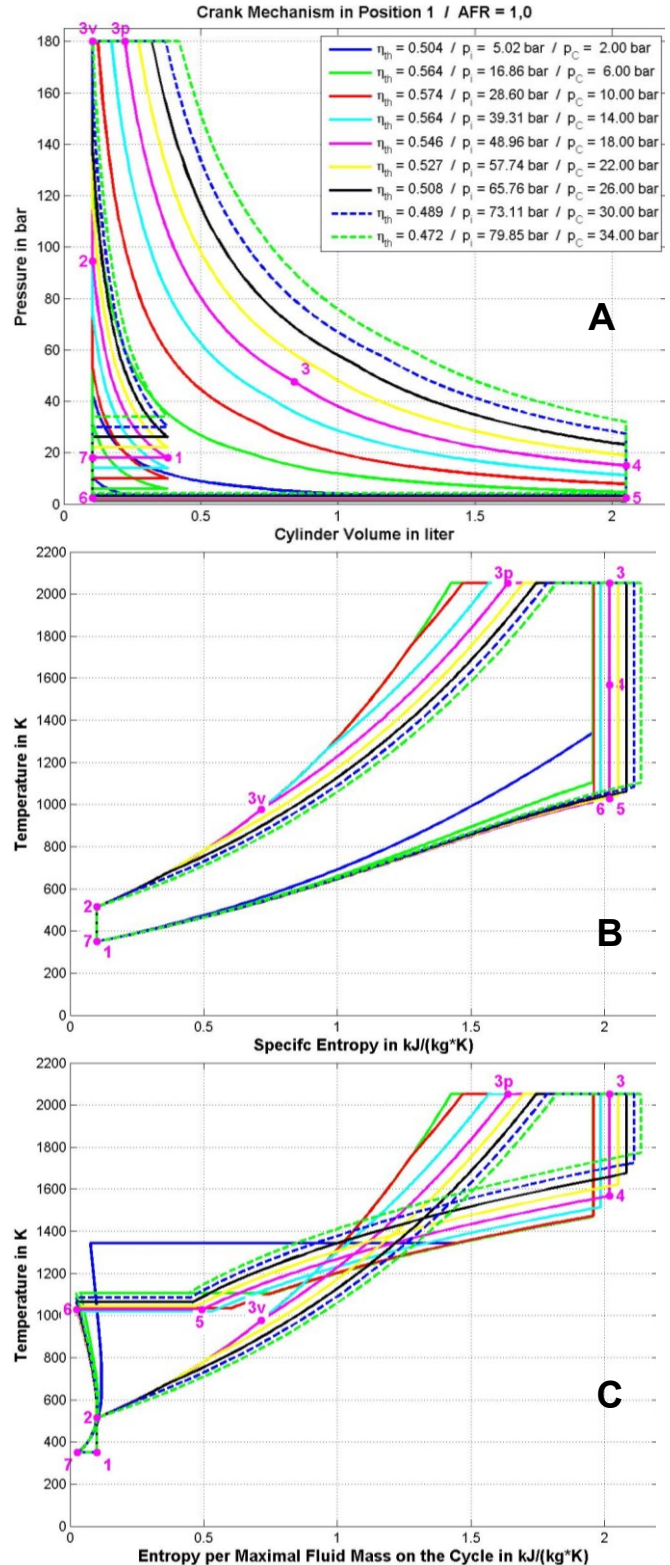
**Figure 12.** Relative Piston Displacement – CA Diagram of an Asymmetrical Crank Mechanism with Variable VCR

The states 1 to 7 marked on the magenta cycle in the three diagrams of the Figure 13 correspond to an 18 bar boost pressure. The red cycle corresponds to a 10 bar boost pressure and has the best TCE for this crank mechanism position. The  $T,s$  diagram from **B**, and more evidently the  $T,s^*$  diagrams from **C**, confirm that this cycle has the highest TCE.

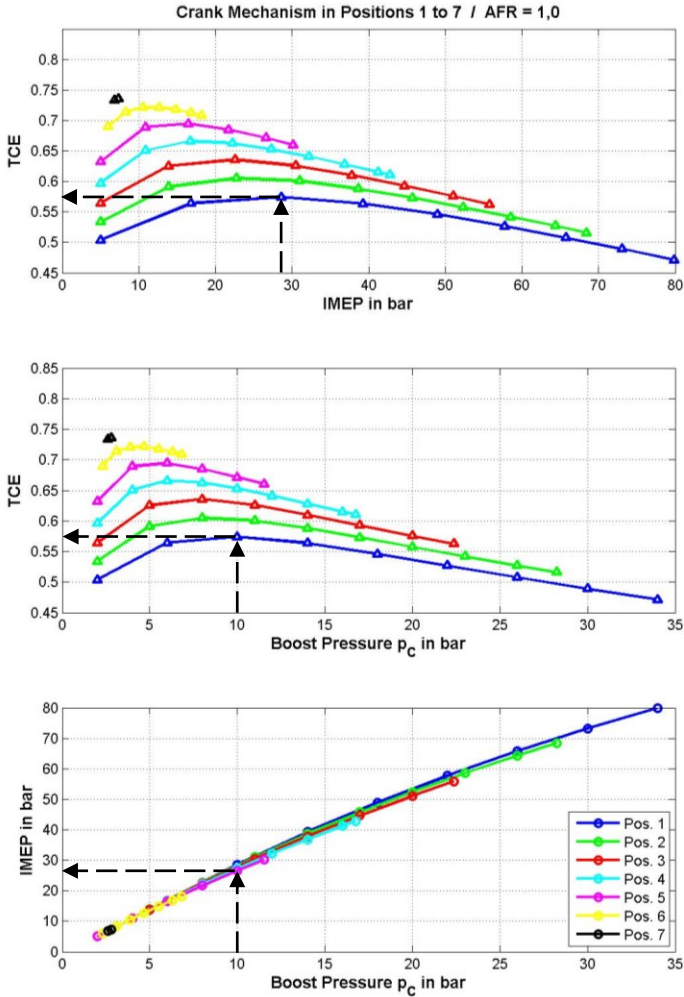
Figure 14 depicts the correlations between TCE, IMEP, boost pressure and crank mechanism positions for the stoichiometric AFR. The arrows show such correlation for position 1 of the crank mechanism where the TCE reaches its maximum. The boost pressure was not limited in these simulations to the current usual maximum values. Whether or not such high boost pressure values are at present achievable is not the subject of this investigation and therefore not discussed here.

Figure 15 presents the corresponding combinations of the heat release fractions for achieving the performances from Figure 14. The isochoric fractions of the released heat are highest (as expected for reaching the maximum of TCE) for the lowest part load in all positions of the crank mechanism, with the exception of 7. This level of the isochoric fractions cannot be maintained in all other EOPs because of the  $p_{max}$  restriction.

An imaginary curve, which tops all the TCE-IMEP curves of the Figure 14 diagram, shows, for example, that the TCE remains much higher than 60% in the case of IMEP values ranging between 5 and 40 bar for stoichiometric AFR, when the crank mechanism position is changing continuously from 7 to 4 and the boost pressure changes accordingly between 2 and 15 bar.



**Figure 13.** **A** represent Pressure-Volume ( $p,V$ ), **B** Temperature-Specific Entropy ( $T,s$ ) and **C** Temperature-Entropy per Max. Fluid Mass diagrams ( $T,s^*$ ) for Crank Mechanism in Position 1 at many Loads with AFR = 1



**Figure 14.** Correlation between TCE, IMEP, Boost Pressure and Crank Mechanism Positions at Full and many Part Loads with Stoichiometric AFR

The increase of the AFR from 1 (i.e. stoichiometric) to 1.5, for example, should theoretically improve the TCE values because the load decreases. That behavior is confirmed in Figure 16. Because less heat is available on the cycle when AFR = 1.5, this heat may be released only isochorically and isobarically without exceeding the limits  $p_{max}$  and  $T_{max}$ . As a result the TCE values are higher for this leaner mixture than in the stoichiometric case (see Fig. 14 and 16).

The question here is whether the exhaust gas energy for turbocharging is sufficient for achieving the required high boost pressure. Figures 17 and 18 depict the pressure and temperature of exhaust gases before turbine and the relative energy balance on the turbocharger for stoichiometric and AFR = 1.5. The values of the isentropic efficiency of compressor and turbine used in these simulations are  $\eta_{sc} = 0.75$  and  $\eta_{sT} = 0.65$ .

The Relative Energy for Turbocharging (RE4T) is defined as the quotient of a) the difference of the works of turbine and

compressor and b) the piston work on the cycle (all these works are considered positive here).

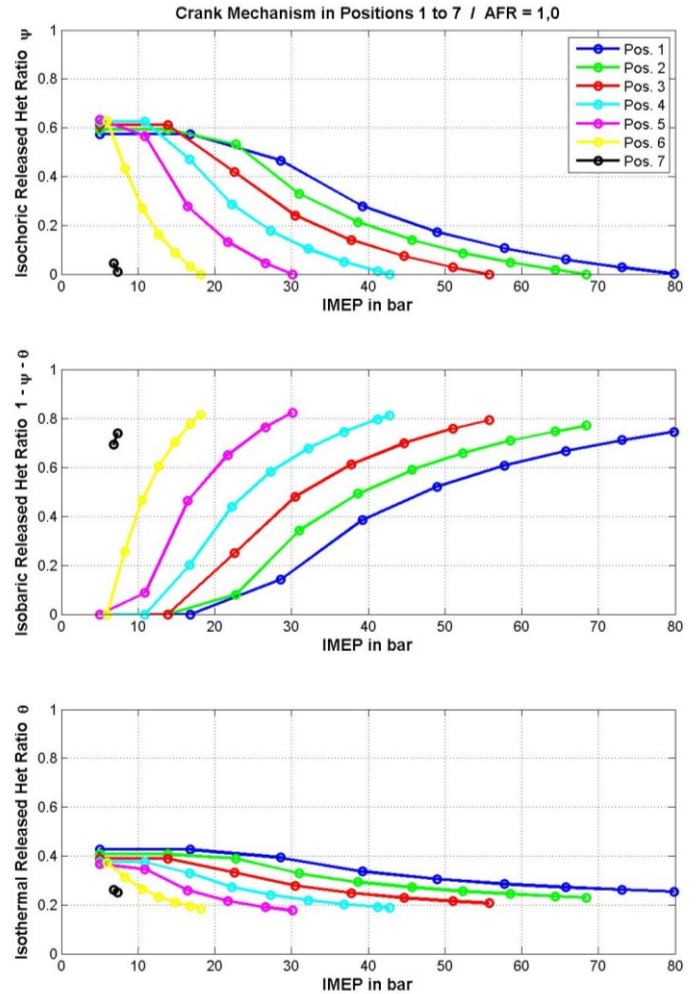


**Figure 15.** Heat Release Fractions - IMEP Diagrams for many Crank Mechanism Positions (see Fig. 12) at Full and many Part Loads with Stoichiometric AFR

The variations of RE4T are depicted in the bottom diagrams of Figures 17 and 18, where the positive values show that the requirement for turbocharging (see Appendix, 5th requirement) is met. The cycles with positive values of RE4T are marked by triangles in the Figures 14 and 16. The other cycles (marked by circles) cannot be realized without the use of a supplementary mechanical compressor.

We can conclude that, for the stoichiometric AFR, that the exhaust gases have enough energy (better said enthalpy) for realizing the necessary boost pressure in all EOP from Figure 14. In the case of AFR = 1.5, the enthalpy of the exhaust gases is sufficient only for a few points at lower part load (see **A** area in Fig. 18).



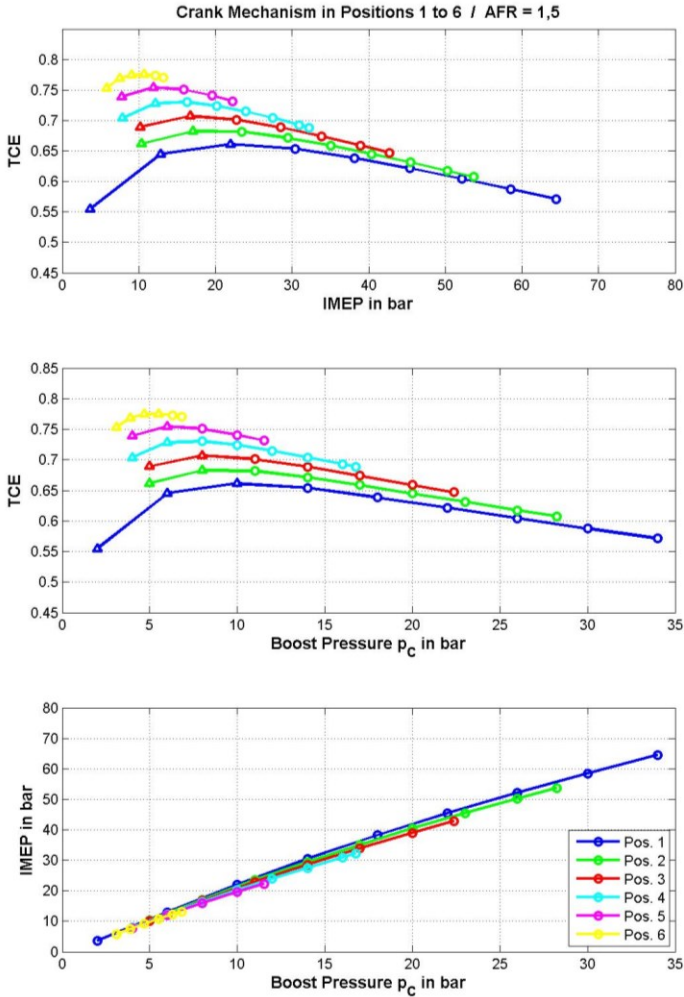


**Figure 16.** Correlation between TCE, IMEP, Boost Pressure and Crank Mechanism Positions at Full and many Part Loads with AFR = 1.5

## CONCLUSION

The TCE gain of the Atkinson cycle implementation on **aspirated engines** - like Toyota has done in Prius II - by means of delaying the intake valve closing and by increasing the VCR is modest and largely dependent on the fine tuning of all control parameters (valve timing etc.). In addition, the specific power of the engine is low because of the lower retained mass of fresh charge in the cylinder before compression. For these reasons, this implementation of the Atkinson cycle is suitable only for hybrid vehicles, where the engine - because it is not directly linked mechanically to the wheels - works only in its best operating range and in combination with an electric motor.

The simulation results for the Atkinson cycle implementation on **supercharged engines**, where the intake valve closing is 60°CA delayed, shows that, although the boost pressure is 40% higher, TCE and IMEP are 6% lower than in

the standard version. In addition, the implementation of the Atkinson cycle by means of an important delaying of the suction and strong enhancement of the charge pressure is investigated. Although the boost pressure in this Atkinson cycle implementation is more than five times higher at nearly the same IMEP, the improvement of the TCE is minor.

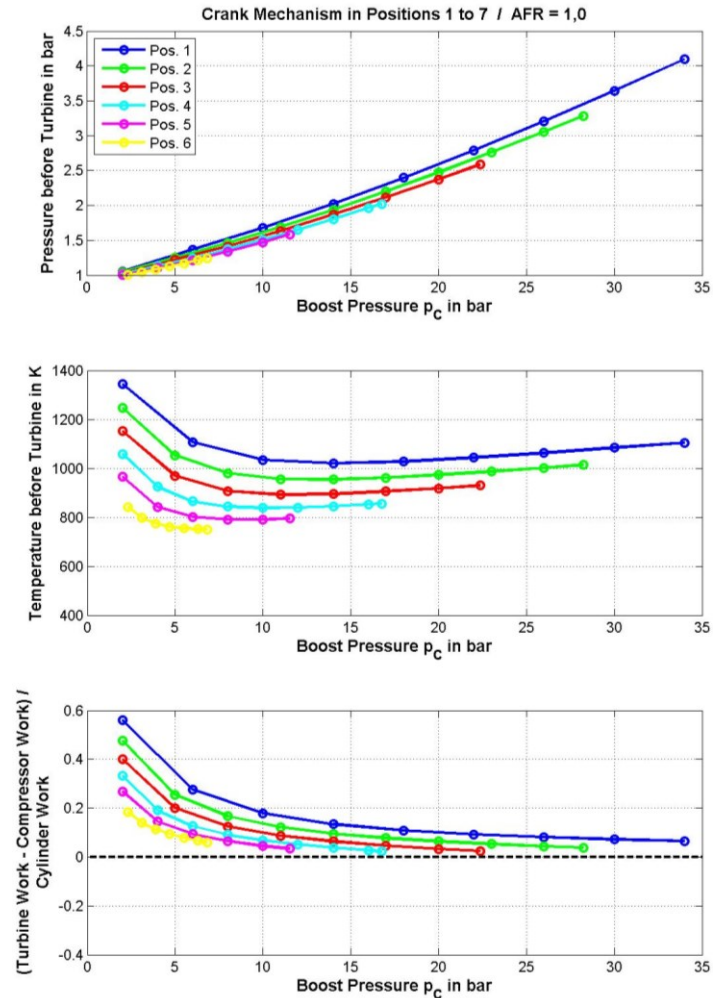


**Figure 17.**  $p_T$ ,  $T_T$  and RE4T - Boost Pressure Diagram for seven Crank Mechanism Positions at Full and many Part Loads with stoichiometric AFR

For these reasons, a new approach is needed to implement a **real Atkinson cycle** on aspirated and supercharged engines. In order to realize a strict Atkinson cycle - i.e. shortened compression and extended expansion - a special crankshaft drive is proposed, which permits geometrically different strokes for compression and expansion.

The analysis of the simulation results for the implementation such Atkinson cycles on **aspirated engines with an asymmetrical crank drive** shows that a 15% increase of IFCE can be achieved.

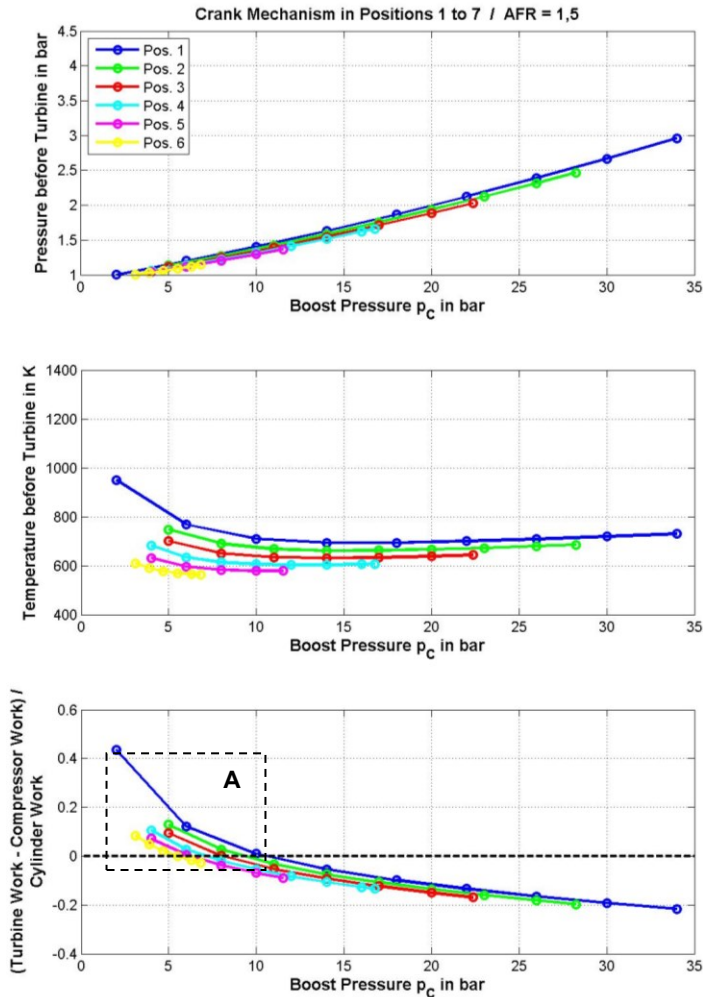


**Figure 18.**  $p_T$ ,  $T_T$ - and RE4T - Boost Pressure Diagram for six Crank Mechanism Positions at Full and many Part Loads with AFR = 1.5

In the case of **supercharged engines**, the number of parameters which influence the TCE becomes much higher. As a consequence, the effort to achieve combinations of parameters which maximize the TCE of **real ICE cycle** becomes much more difficult. For these reasons, **ideal models of the V,p,T-Seiliger and -Atkinson cycles** are developed for this purpose (see Appendix).

The TCE of the Atkinson cycle implemented at **supercharged engines with asymmetrical crank drive** is more than 25% better and the IMEP exceeds by more than 70% that of the Seiliger cycle, while meeting the same mechanical and thermal limits in both cycles.

The implementation of the Atkinson cycle by means of the asymmetrical crank drive has the disadvantage that at part loads - because of the very extensive expansion - the cycle stops being feasible, i.e. the pressure at the end of expansion becomes lower than the ambient pressure (see Appendix, Requirements for cycle realization). For this reason, an asymmetrical crank

mechanism which also enables the variation of the VCR is needed.

With such a crank mechanism it is possible to realize Atkinson cycles for part loads even with stoichiometric AFR and without throttling.

## REFERENCES

1. Heywood, JB, Internal Combustion Engine Fundamentals, MacGraw-Hill Book Company, 1988
2. Pischinger, A, Kraßnig, G, Taucar, G, & Sams, Th., Thermodynamic of Internal Combustion Engines (German), Springer-Verlag, Wien New York, 1989
3. Muta, K., Yamazaki, M. Tokieda, J., [Development of New-Generation Hybrid System THS II - Drastic Improvement of Power Performance and Fuel Economy](#), SAE 2004-01-0064 and Toyota Hybrid System (THS) II, Toyota Motor Corporation, Public Affairs Division, Japan, 2003
4. Gheorghiu, V, [Enhancement Potential of the Thermal Efficiency of ICE Cycles Especially for Use into Hybrid Vehicle](#), HEFAT 2007, 5th International Conference on Heat Transfer, Fluid Mechanics and Thermodynamics, Paper number: GV1, July 2007, Sun City, South Africa
5. Gheorghiu, V, [Higher Accuracy through Combining of quasi-3D \(instead of 1D\) with true-3D Manifold Flow Models during the Simulation of ICE Gas Exchange Processes](#), 2001-01-1913, SAE Congress, Orlando, Florida, USA, 2001
6. Gheorghiu, V, [Simulation Results of Compressible Unsteady Flows Through ICE Manifolds](#), F2004F427, FISITA Congress, Barcelona, Spain, 2004
7. Schutting, E, Neureiter, A, Fuchs, Ch., Schwarzenberger, T, Klell, M, Eichlseder, H, Kammerdiener, T, Miller- and Atkinson-Cycle for Supercharged Diesel Engines, MTZ 06 / 2007 (German)
8. Gheorghiu, V, [CO2-Emission Reduction by means of Enhanced Thermal Conversion Efficiency of ICE Cycles](#), ICE200 09ICE-0130 / SAE 2009-24-0081, ICE, Neapel, Italy, 2009

## DEFINITIONS

Symbol	Meaning	Units
$\varepsilon_c = \frac{V_1}{V_2} = \frac{V_{in}}{V_c}$	volumetric compression ration	-
$\varepsilon_e = \frac{V_5}{V_2} = \frac{V_e}{V_c}$	volumetric expansion ratio	-
$V_{in} = V_1$	cylinder volume at end of suction	m <sup>3</sup>
$V_c = V_2 = V_{3v}$	cylinder volume at end of compression	m <sup>3</sup>
$V_e = V_4 = V_5$	cylinder volume at end of expansion	m <sup>3</sup>
$V_{out} = V_6 = V_7$	cylinder volume at end of emptying	m <sup>3</sup>
$V_{max} = V_4 = V_5$	maximal cylinder volume	m <sup>3</sup>
$p_{max} = p_{3v} = p_{3p}$	maximal pressure on cycle	Pa
$p_{max.0}$	desired value of $p_{max}$	Pa
$p_{max.\psi 1}$	$p_{max}$ for 100% isochoric heat release	Pa
$p_C = p_1$	charge pressure after cooler	Pa
$p_{C.0}$	desired value of $p_C$	Pa
$p_T$	pressure before turbine	Pa
$T_C = T_1$	charge temperature after cooler	K
$T_{C.0}$	desired value of $T_C$	
$T_{max} = T_{3p} = T_3$	maximal temperature on cycle	K
$T_{max.\psi 1}$	$T_{max}$ for 100% isochoric heat release	K
$m_a$	fresh charge mass per cycle	kg
$m_1 = m_a \cdot \varepsilon_a$	cylinder gas mass in state 1	kg
$m_f$	fuel mass per cycle	kg
$\kappa = \frac{c_p^\circ}{c_v^\circ}$	isentropic exponent	-
$c_p^\circ, c_v^\circ$	isobaric & isochoric specific heat capacity	$\frac{J}{kg \cdot K}$
$\lambda$	air-fuel ratio (AFR)	-
$L_{st}$	stoichiometric air requirement ratio	$\frac{kg \cdot air}{kg \cdot fuel}$
$H_u$	fuel lower heating value	$\frac{J}{kg}$
$q_{zu} = \frac{\eta_b \cdot m_f \cdot H_u}{m_1}$	released heat per unit fluid mass	$\frac{J}{kg}$
$\eta_b$	released fuel energy completeness	-

## APPENDIX / FORMULA

### Formula for the ideal V,p,T-model

$$\delta = \frac{H_u \cdot \eta_b}{\lambda \cdot L_{st} \cdot c_v^\circ \cdot T_C \cdot \varepsilon_a}$$

$$\varepsilon_a = \frac{\frac{V_{in}}{V_{out}}}{\frac{V_{in}}{V_{out}} - 1}$$

$$p_C = \min\left(p_{C.0}, \frac{p_{max.0}}{\varepsilon_c^\kappa}\right)$$

$$T_{max.\psi 1} = T_C \cdot (\varepsilon_c^{\kappa-1} + \delta)$$

$$T_{max} = \min(T_{max.0}, T_{max.\psi 1})$$

$$p_{max.\psi 1} = p_C \cdot (\varepsilon_c^\kappa + \delta \cdot \varepsilon_c)$$

$$\psi_{Tmax} = \frac{1}{\delta} \cdot \left( \frac{T_{max.0}}{T_C} - \varepsilon_c^{\kappa-1} \right)$$

$$\psi_{pmax} = \frac{1}{\varepsilon_c \cdot \delta} \cdot \left( \frac{p_{max.0}}{p_C} - \varepsilon_c^\kappa \right)$$

$$\psi = \min(\psi_{Tmax}, \psi_{pmax}, 1)$$

$$p_{max} = p_C \cdot \varepsilon_c \cdot (\varepsilon_c^{\kappa-1} + \psi \cdot \delta)$$

$$\theta = 1 - \psi - \frac{\kappa}{\delta} \cdot \left( \frac{T_{max}}{T_C} - \varepsilon_c^{\kappa-1} - \psi \cdot \delta \right)$$

$$\theta = \max(\theta, 0)$$

$$a = \frac{\varepsilon_c^{\kappa-1}}{\delta} + \psi + \frac{1 - \psi - \theta}{\kappa}$$

$$T_{max} = a \cdot T_C \cdot \delta$$

$$b = 1 + \frac{(1 - \psi - \theta) \cdot \delta}{\kappa \cdot (\varepsilon_c^{\kappa-1} + \psi \cdot \delta)}$$

$$\eta_{th} = \frac{1}{\delta} \cdot \left[ 1 - \varepsilon_c^{\kappa-1} + \frac{\kappa-1}{\kappa} \cdot (1 - \psi) \cdot \delta + \frac{\theta \cdot \delta}{\kappa} \dots \right] \dots$$

$$+ a \cdot \left[ 1 - \left( \frac{b}{\varepsilon_e} \right)^{\kappa-1} \cdot \exp\left(\frac{\theta}{a}\right) \right]$$



Symbol	Meaning	Units
$\delta = \frac{q_{zu}}{c^{\circ}_v \cdot T_1}$	relative released heat as measure of engine load	-
$q_{zu,v}$	isochoric part of $q_{zu}$	$\frac{J}{kg}$
$\psi = \frac{q_{zu,v}}{q_{zu}}$	isochoric released heat fraction	-
$q_{zu,t}$	isothermal part of $q_{zu}$	$\frac{J}{kg}$
$\theta = \frac{q_{zu,t}}{q_{zu}}$	isothermal released heat fraction	-
$1 - \psi - \theta$	isobaric released heat fraction	-
$\phi = \frac{p_T}{p_C}$	turbine to compressor pressure ratio	-
$\eta_{th} = \frac{-W_{cycle}}{q_{zu}}$	thermal conversion efficiency	-
$W_{cycle}$	specific work on the all cycle	$\frac{J}{kg}$
$p_i = IMEP$	indicated mean pressure	bar
$\eta_{sC}, \eta_{sT}$	isentropic efficiency of compressor and turbine	-
$W_{TTu}$	turbine work between $p_T$ and $p_u$	J
$W_{CuC}$	compressor work between $p_u$ and $p_C$	J
$io, ic$	intake valve open & close locations	
$eo, ec$	exhaust valve open & close locations	
$u$	ambient state index	

## ABBREVIATIONS

<b>AFR</b>	Air-Fuel Ratio
<b>CA</b>	Crank Angle
<b>EOP</b>	Engine Operating Point
<b>ICE</b>	Internal Combustion Engine
<b>IFCE</b>	Indicated Fuel Conversion Efficiency
<b>IMEP</b>	Indicated Mean Pressure
<b>RE4T</b>	Relative Energy for Turbocharging
<b>SI</b>	Spark Ignition Engine
<b>TCE</b>	Thermal Conversion Efficiency
<b>VCR</b>	Volumetric Compression Ratio
<b>SV</b>	Standard Variant for Aspirated Engine
<b>2V</b>	Second Variant for Aspirated Engine
<b>3V</b>	Third Variant for Aspirated Engine
<b>1V-TC</b>	First Variant for Turbo Charged Engine
<b>2V-TC</b>	Second Variant for Turbo Charged Engine
<b>io</b>	Intake Valve Open
<b>ic</b>	Intake Valve Close
<b>eo</b>	Exhaust Valve Open
<b>ec</b>	Exhaust Valve Close

## Formula for the ideal V,p,T-model

$$T_4 = T_{max} \cdot \left[ \frac{a \cdot \delta}{\varepsilon_e \cdot (\varepsilon_c^{\kappa-1} + \psi \cdot \delta)} \right]^{\kappa-1} \cdot \exp\left(\frac{\theta}{a}\right)$$

$$T_T = T_4 \cdot \left( \frac{p_T}{p_C} \cdot \frac{T_C}{T_4} \cdot \frac{\varepsilon_e}{\varepsilon_c} \right)^{\frac{\kappa-1}{\kappa}}$$

$$p_4 = p_C \cdot \frac{T_4}{T_C} \cdot \frac{\varepsilon_c}{\varepsilon_e}$$

$$p_T = p_u + \frac{p_4 - p_u}{10} \quad (\text{hypothetical})$$

$$W_{TTu} = \eta_{sT} \cdot (m_a + m_f) \cdot c^{\circ}_p \cdot T_T \cdot \left( 1 - \frac{T_u}{T_T} \right)$$

$$W_{CuC} = \frac{m_a \cdot c^{\circ}_p \cdot T_u}{\eta_{sC}} \cdot \left[ \left( \frac{p_C}{p_u} \right)^{\frac{\kappa-1}{\kappa}} - 1 \right]$$

## Requirements for cycle realization

### 1. Requirement (for maximal pressure)

$$p_{max} \geq p_C \cdot \varepsilon_c^{\kappa} \quad \text{i.e.} \quad \psi \geq 0$$

$$p_{max} \leq p_C \cdot \varepsilon_c \cdot (\varepsilon_c^{\kappa-1} + \delta)$$

### 2. Requirement (for maximal temperature)

$$T_{max} \geq T_C \cdot \varepsilon_c^{\kappa-1}$$

$$T_{max} \leq T_C \cdot \left( \varepsilon_c^{\kappa-1} + \psi \cdot \delta + \frac{\delta}{\kappa} \right)$$

### 3. Requirement (for heat release)

$$1 - \psi - \theta \geq 0 \quad \text{and} \quad \theta \geq 0$$

### 4. Requirement (for expansion)

$$p_4 > p_u$$

### 5. Requirement (for turbocharging)

$$W_{TTu} > W_{CuC}$$

$$p_T > p_u$$